A Signal Level Simulator for Multistatic and Netted Radar Systems

MARC BROOKER, Member, IEEE
MICHAEL INGGS, Member, IEEE
University of Cape Town

Efficient analysis of modern multistatic and netted radar systems requires a new generation of dedicated radar simulation software. Key requirements for such software are simulation accuracy and flexibility in choosing system parameters. In this paper, algorithms for the simulation of raw radar return signals are presented based on interpolation and modification of the transmitted signal and modelling of the radar hardware and environment. This method supports simulation of pulsed and CW systems; monostatic, multistatic, and netted systems; phased-array radars; and most physically realizable radar system configurations.

Manuscript received February 15, 2008; revised November 30, 2008; released for publication August 1, 2009.

IEEE Log No. T-AES/47/1/940023.

Refereeing of this contribution was handled by Y. Abramovich.

This work was supported by the South African National Defence Force.

Authors' address: Dept. of Electrical Engineering, University of Cape Town, Private Bag, Rondebosch, 7701, South Africa, E-mail: (marcbrooker@gmail.com).

I. INTRODUCTION

The ability to simulate the performance of a radar system early in the design life cycle is becoming increasingly important due to increases in system complexity and demand for radar systems that offer excellent performance at a low cost. Analysis of simple monostatic radar systems is well understood and can be performed without the assistance of specialised software [1]. In contrast, the analysis of complex radar systems is often intractable without the application of a dedicated radar simulation system.

Recent research into radar simulation has focused primarily on simulators for specific types of radar systems such as synthetic aperture radar (SAR) and moving target indication (MTI) systems. While special purpose simulators ([2] and [3], for example) are extremely useful in particular fields, the development of a general purpose simulator applicable to many types of radar systems (including future systems) is interesting. Many past flexible simulators (such as [4]), while suited to the simulation of traditional radar applications, have severe limitations such as the inability to simulate multistatic and CW radars.

This paper presents the design of general purpose software for the digital simulation of raw radar return signals based on the modelling of radar hardware and the environment and the modification of the transmitted signal using digital signal processing (DSP) techniques. The simulator has been designed for the accurate simulation of raw returns in complex, multistatic, and netted radars and is applicable to pulsed and continuous wave (CW) systems as well as both active and passive radar systems. In addition, active and passive electronically scanned array designs are supported. The algorithm is expected to be especially valuable for the simulation of emerging radar technologies, such as passive coherent location [5, 6] (PCL), netted radar [7, 8] and phased-array radar.

This paper describes the algorithms and models used for simulation, discusses their implementation, and compares simulation results with measured returns from the NetRad experimental netted radar system [7, 8], and theoretical predictions of MTI radar performance.

II. RADAR SIMULATION MODEL

It is a convenient simplification to model the radar return signal as the sum of multiple independent target returns. In a simulated scene with T transmitters and S scatterers, the discrete-time return signal to the receiver r, $y_r[k]$ can be modelled as the sum of N responses (1) where $N = T(S + 1)$. This simplification allows each scatterer to be considered independently,

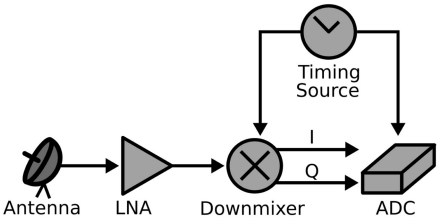

Fig. 1. Functional model of receiver hardware.

greatly reducing the complexity of the calculations required to simulate the return signal.

$$y_r[k] = \sum_{i=0}^{N} s_i[k]. \tag{1}$$

The scatterer returns $s_i[k]$ are modelled as copies of the transmitted signal $x[k]$ which have been modified by the effects of transmission, propagation, interaction with the scatterer, and reception. The signal $s_i[k]$ can therefore be expressed as the product of three processes which modify the transmitted signal $x(n)$: transmission ($H_t(x)$), environmental interaction ($E(x)$), and reception ($H_r(x)$).

$$y[k] = \sum_{i=0}^{N} H_r(E(H_t(x[n]))). \tag{2}$$

The radar simulation problem is equivalent to finding the functions $H_t(x)$, $E(x)$, and $H_r(x)$, understanding how these functions affect the transmitted signal, and applying these effects to copies of the transmitted signal. In the simulator described here, the hardware simulation functions $H_t(x)$ and $H_r(x)$ are derived from a parametric hardware model, and the environment interaction function $E(x)$ is derived from an environment model. The effects of these functions are applied to the transmitted function using DSP techniques.

A. Radar Hardware Models

The radar hardware model is based on two parametrized functional hardware models. The receiver model, as illustrated in Fig. 1, consists of a receive antenna, amplifier, quadrature downmixer, and signal capture hardware. The transmitter model is similar to the receiver model and consists of a signal source, quadrature upmixer, amplifier, and transmission antenna. Both models include a timing source which provides time and frequency information to the other blocks, and both consider the effects of imperfections in the timing information received from this source.

The parameters of each functional block in the hardware model are changed to reflect the performance of the hardware of the system under simulation. Each functional block includes multiple tunable parameters, for example, gain, noise temperature, and bandwidth in the amplifier blocks and the shape and amplitude of the phase noise curve for timing blocks. This functional model is sufficiently flexible to describe the performance of a large number of modern radar system designs.

B. Modelling the Effects of System Hardware

The effects of transmission ($H_t(x)$) and reception ($H_r(x)$) on the radar signal are calculated using the hardware model.

The intended effects of the transmission chain are to produce an analog signal, upmix it to the required transmission frequency, amplify it to the required transmission power, and transmit it using the required antenna gain pattern. The intended effects of transmission are therefore gain (from the amplifier and antenna) and the upmixing of the inphase and quadrature parts of the transmitted signal to a higher frequency. The unintended effects of transmission are linear effects (nonflat frequency response, etc.), nonlinear effects (amplifier distortion, digital-to-analog conversion (DAC) distortion, and timing source phase noise effects), and the addition of noncorrelated noise.

The intended effects of reception are to add gain to the signal (from the antenna and front-end amplifier), downmix the signal to IF or baseband, and possibly convert the signal into a stream of digital samples. Unintended effects of reception are similar to those of transmission, but also include the addition of distortion and quantization noise in the analog-to-digital converter (ADC). Where the radar hardware of interest performs more complex operations, such as beam forming and filtering, these operations can be included in the hardware modelling functions $H_t(x)$ and $H_r(x)$.

C. Radar Environment Model

1) *The Object Model*: The environment model of the simulator recognises three kinds of objects: transmitters, receivers, and scatterers and accepts any number of each type of object in arbitrary geometric configurations. In addition, the model can include a single surface which reflects radar energy for the simulation of specular multipath propagation. Each object in the environment is assigned a spatial position, path of motion through space, and rotation. Positions, velocities, and paths can be assigned exact values or statistical distributions of values.

Each transmitter in the model is independently assigned a waveform to transmit, an associated hardware model, and a transmission schedule. The transmission schedule models the pulse repetition frequency (PRF) of the transmitter. The transmitter object is intended to be used to model radar transmitters, the transmission part of monostatic radars, transmitters of opportunity (such as FM towers), noise sources, and active electronic warfare (EW) systems.

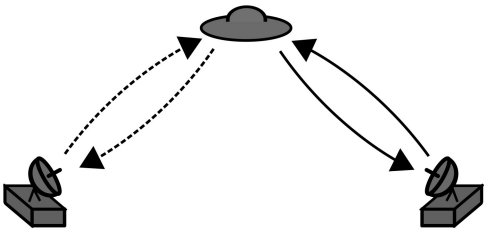

Fig. 2. Monostatic return paths in bistatic radar system.

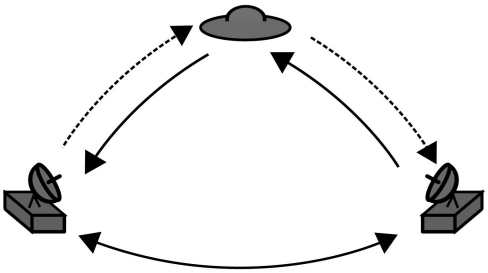

Fig. 3. Multistatic and direct return paths in bistatic radar system.

Receivers in the model are independently assigned a hardware model and receive schedule. The receive schedule is used to model range gating and can be slaved to the schedule of an associated transmitter. The receiver object models radar receivers and the reception part of monostatic radars.

Scatterers in the model are independently assigned monostatic or bistatic radar cross sections (RCS) and are used to model both intended targets, unintended targets (clutter) and mechanical jamming (chaff, etc.). Currently only point scatterers with arbitrary RCSs are supported. Note that this model does not make a distinction between intended targets and unintended targets (clutter)—the effects on the radar signal of both of these types of scatterers are the same.

2) *Responses*: Using the number of transmitters, receivers and targets in the environment, the model calculates the total number of responses for each transmitted pulse. In multistatic systems, monostatic (Fig. 2), multistatic (Fig. 3), and direct return paths are included in the total number of pulses. The presence of a multipath surface increases the number of responses as reflection paths are added to each bistatic pair.

In a multistatic radar system, the total number of returns per pulse seen by each receiver in a system with T transmitters, P targets, and S multipath simulation surfaces is $RT(P+1)(S+1)$. Each of these returns can be considered independently and summed for each receiver, as in (1). This number is an upper bound on the number of responses—in some systems responses may be lost due to range gating, the effects of antenna gain patterns, and propagation effects.

Multiscatter (return paths which contain more than one scatterer) are not included in the calculation of N in Section II. Low-order mulitscatter paths can be included directly in the calculation of (2) by extending $E(x)$ to consider the effects of interaction with all targets on the path. The extension of (1) to a complete global illumination model (see [9], for example) would be required to consider higher order multiscatter paths, as direct calculation of these paths with (2) would not be computationally efficient.

D. Propagation Effects

Propagation through the atmosphere has two major effects on signals transmitted at common radar frequencies: delay and attenuation.

The effects on the received radar signal due to the delay caused by propagation can be decomposed into two effects: a phase shift on the carrier (phase delay) and a time shift of the envelope of the transmitted signal (group delay), assuming that the transmitted signal consists of a complex bandlimited signal that is mixed with a carrier at a constant frequency. Considering these two effects separately simplifies the computational task of signal processing as the computationally complex group delay simulation only needs to be applied to the baseband signal.

Most simulators described in the literature assume that the phase and group delay are constant throughout each pulse ([4], for example) and that motion occurs during the inter-pulse interval. This stop-go assumption is only valid for radar systems with short pulses and those where the target range is changing slowly. The maximum allowable simulation error depends on the type of processing used on simulation results. Doppler velocitometry techniques, for example, do not consider the change of phase and group delay over the pulse interval, making the errors introduced by assuming stop-go behaviour irrelevant.

The second major effect of signal propagation through the atmosphere is attenuation. The power of the return signal, for the case where the signal bandwidth is much less than the carrier frequency, can be computed using the radar (3) for target reflections and (4) for direct return paths [1].

$$P_r = \frac{P_t G_t G_r \rho_b \lambda^2}{(4\pi)^3 R_t^2 R_r^2} \tag{3}$$

and

$$P_r = \frac{P_t G_t G_r \lambda^2}{(4\pi)^3 R^2} \tag{4}$$

where P_t is the transmitted power, G_t and G_r are the gain of the transmit and receive antennas in the direction of the target, λ is the carrier wavelength, and R, R_t, and R_r are the lengths of the direct path, transmitter-target path, and target-receiver path, respectively. ρ_b is the bistatic RCS of the target corresponding to the arrival and departure angles. For monostatic paths, (3) is used, with $R_t = R_r$ and ρ_b equal to the monostatic RCS.

For wideband signals, the return strength is frequency dependent. In this case, a linear phase digital filter matching $P_r \propto \lambda^2$ is designed using the fast Fourier transform (FFT) and applied to the signal.

The radar equation provides a simple calculation for the power of the return signal, but does not include attenuation due to atmospheric factors. Attenuation due to propagation through the atmosphere is frequency dependent and varies widely across commonly used radar bands. The attenuation coefficient can be found in many standard references (such as [1]) and multiplied by the propagation distance (R or $R_t + R_r$) to find the attenuation due to atmospheric propagation.

This model is not limited to the linear phenomena of attenuation and delay. In order for the calculation in (2) to be valid, the propagation medium must be linear. It is not assumed, however, that the permittivity (ϵ) and permeability (μ) of the medium are constant and scalar. The environment model can include effects such as dispersion (where ϵ and μ are functions of frequency) and anisotropy (where ϵ and μ are second-rank tensors).

III. SIGNAL PROCESSING

Following the identification of the simulation transfer functions H_t, H_r, and E, DSP approaches are used to modify the transmitted signal to match the expected parameters of the received signal.

A. Phase Delay and Doppler Shift

The phase of the carrier at the receiver is determined by the signal propagation time. Where this time is not constant, the changing phase shift is seen as a frequency or Doppler shift on the received signal. In this simulation, the per-sample phase shift $\varphi(t)$ is calculated from the carrier frequency and bistatic range of the transmitter, target, and receiver using standard relativistic Doppler calculations. Considering the phase effects of propagation as a per-sample phase shift $\varphi(t)$ rather than a fixed frequency shift, allows the model to offer per-sample Doppler accuracy without making assumptions about the speed of target movement or the length of pulses.

Using a relativistic model to consider the phase shift introduces further accuracy by relaxing the assumption that targets are moving at a small fraction of the speed of propagation.

The inphase I and quadrature Q parts of the downmixed return pulse are calculated from $\varphi(t)$ and the real and complex parts of the transmitted pulse.

$$I[k] = \tfrac{1}{2}\mathcal{R}(y[k])\cos(\phi) - \tfrac{1}{2}\mathcal{I}(y[k])\sin(\phi) \quad (5)$$

$$Q[k] = \tfrac{1}{2}\mathcal{R}(y[k])\sin(\phi) + \tfrac{1}{2}\mathcal{I}(y[k])\cos(\phi) \quad (6)$$

where $\mathcal{R}(x)$ and $\mathcal{I}(x)$ are the real and imaginary part of x, respectively, and $\phi = \varphi(k/f_0)$.

B. Group Delay

The application of time-dependent group delay to a digital signal requires a tradeoff to be made between computational speed and accuracy. For constant group delay of an integer number of samples, the sample stream can simply be shifted. For noninteger delays, simulation of group delay requires interpolation of the samples.

Finite impulse response (FIR) fractional delay filters, based on windowed truncation of the ideal bandlimited interpolation [10] filter, are used to apply time-dependent group delay to discrete-time signals. The exact values of the samples of the delayed signal $d_i[k]$ (properly sampled at f_0 Hz) can be calculated from the transmitted signal $x[n]$ and the time-dependent delay function $T_d(t)$ using the summation in (7) [11]

$$d_i[k] = \sum_{n=-\infty}^{\infty} x[n] h_s\left(k - T_d\left(\frac{n}{f_0}\right) - n\right) \quad (7)$$

$$h_s(t) = \frac{\sin(\pi t)}{\pi t}. \quad (8)$$

If the delay function is not constant, the delayed signal $d_i[k]$ undergoes an apparent shift in frequency. In cases where the frequency shift causes a net increase in frequency, it is critical that the sample rate f_0 is sufficiently high that the delayed signal $d_i[k]$ is properly sampled, or distortion will occur due to aliasing.

The process described in (7) can be understood as convolution of the transmitted signal with a digital filter with the required group delay. The filter function $h_s(t)$ cannot be precomputed as the group delay is time varying.

1) *Implementation of Group Delay Algorithm*: A direct implementation of the summation (7) is impractical as it requires $O(N^2)$ operations for $x[n]$ with length N. Evaluating (7) using a FIR approximation of the ideal interpolation filter (8) reduces the runtime to $O(N)$ at the cost of numerical accuracy.

Simple truncation of the filter function $h_s(t)$ will severely reduce the stopband attenuation of the interpolation function, increasing distortion and aliasing. This effect can be effectively reduced by the application of a suitable window function to $h_s(t)$ prior to truncation. The Kaiser window [12, 13] is ideal for this application [14], as the compromise runtime, flatness of the passband, and bandwidth can be adjusted with the window parameters β and N without changing the algorithm implementation. The desired value of β and window width M can be calculated using the method described by Kaiser [12].

Application of the Kaiser window function to truncate $h_s(t)$ to M samples produces (9) to

replace (8)

$$h_s(t) = \begin{cases} \dfrac{\mathrm{w}(|t|)\sin(\pi t)}{\pi t}, & |t| \le M, \\ 0, & \text{otherwise} \end{cases} \tag{9}$$

where $\mathrm{w}(t)$ is the zero-centered Kaiser window function with length M and shape β.

The Kaiser window function is computationally expensive—evaluating it requires two calculations of the value of the zeroth-order modified Bessel function and one square root. In simulations of long periods or high bandwidths, an optimisation of this calculation could be desirable.

The simulated described in this paper uses a twelfth-order polynomial approximation of $I_0(x)$ (from [15]) as the base of an approximation to the true Kaiser window function. The maximum error of this approximation is less than 1.2×10^{-8}. The simulator uses this function to populate a variable sized table of subsample delay filters. The loss in accuracy due to this approach depends on the table size: for a table of 10^5 filters of length 32, the maximum interpolation delay is -83 dB. In cases where this accuracy would limit the dynamic range of the simulation (that is, systems with over 13 bits of dynamic range), the table size can be increased.

C. Addition of Noise and Distortion

The key limiting factor on the performance of radar systems is the signal-to-noise ratio (SNR) of the return signal. It is therefore important to correctly model the noise received along with the return pulse.

1) *Additive Noise*: For narrowband radar systems (where the bandwidth is much smaller than the carrier frequency), the additive noise can be considered Gaussian noise with a constant spectral density. The total system noise consists of the sum of the noise picked up from the environment and the noise created by the transmission and reception systems. For simulation of most practical radar systems, it is sufficient to specify the equivalent system noise temperature, generate bandlimited white Gaussian pseudonoise, and sum it with the return signal.

The system noise temperature depends on the environment, the elevation and gain pattern of antennas, and the noise figure of the amplifiers used in the transmitter and receiver.

2) *Quantisation Effects*: Additional noise and distortion is added by the D/A converter in the transmitter and the A/D converter in the receiver. In practical cases, the effects of A/D conversion can be assumed to be purely additive and the additive noise signal $e[n]$ assumed to be stationary and uncorrelated with the signal being quantised [13, 16]. The signal-to-quantisation noise ratio (SQNR) depends on the properties of the return signal and the sampling rate. For a typical radar signal with bandwidth B, the SQNR can be expressed as

$$\mathrm{SQNR} = 20\log_{10} 2^N + 20\log_{10}\sqrt{\frac{3}{2}} + 10\log_{10}\frac{f_s}{2B} \tag{10}$$

for an N-bit ADC with sampling rate f_s [17].

The simulator directly simulates A/D quantisation effects by truncating simulation results to the required number of bits. This approach, while more computationally expensive than the addition of pseudonoise, offers a more accurate simulation of A/D effects, including the nonlinear effects of quantisation to a small number of bits.

D. Phase Noise and Jitter Effects

Errors in the time and frequency sources in the radar system have several effects on the received signal.

The most obvious effect is the gross errors due to timing inaccuracy which cause incorrect referencing of the time of the received signal compared with the transmission time. The simulator handles these errors by adding random perturbations to the timestamps recorded for received data, corresponding to the jitter on the timing source in the receiver hardware model.

Phase noise on the timing source has an effect on the upmixing and downmixing steps of the hardware model. To simulate these effects, the instantaneous phase deviations in the transmitter (φ_t) and receiver (φ_r) timing sources are added to the phase shift factor φ in (5) and (6). The instantaneous phase deviations φ_r and φ_t are generated from a statistical model of the phase noise present on the timing source. The simulator uses a novel multirate filter structure (described in [18]) to accurately generate samples of phase noise matching the characteristics of the oscillator technology used in the system under simulation.

A third effect of phase noise on the timing sources is a degradation of the performance of the A/D and D/A converters in the receiver and transmitter. Presence of jitter on the data conversion of the clock reduces the SNR of the data converters. An error term is added to the group delay simulation (7) to simulate the effects of jitter on data conversion [19]. Jitter samples are computed from numerical integration of the phase noise model of the timing source [18].

IV. CALCULATING THE RAW RETURN SIGNAL

Using the equations developed above, a complete equation (11) for the samples of the raw radar signal as received by receiver r can be obtained.

$$y_r[k] = \sum_{t=0}^{T} \left(A_{tr}\left(\frac{k}{f_0}\right) d_{tr}[k] + \sum_{p=0}^{P} A_{tpr}\left(\frac{k}{f_0}\right) d_{tpr}[k] \right). \tag{11}$$

In (11) T is the number of transmitters in the radar system and $A_{tr}(x)$ and $d_{tr}[k]$ are the amplitude function and delayed samples for the direct path between transmitter t and receiver r, respectively. The summation across P corresponds to the P targets in the simulated system, with $A_{tpr}(x)$ and $d_{tpr}[k]$ corresponding to the amplitude function and delayed samples for the transmitter-target-receiver path.

A. Computational Complexity

For a simulation based on (11), evaluation of the raw signals for all the receivers in the simulated system requires $R \times T \times S$ evaluations of (7) and (3) for R receivers, T transmitters, and S scatterers.

The most computationally intensive operation required for simulation is the evaluation of (7). Using the windowed representation of $h_s(t)$, (9), evaluation of (7) requires $\mathbf{O}(NM)$ steps for a signal length of N samples and window length of M samples. The window length M is chosen depending on the required simulation accuracy, but in most cases $M \ll N$, and (7) can be considered as running in linear time.

In practically realizable radar systems, T and R will be small constant values. Evaluation of (11) is therefore approximately $\mathbf{O}(SN)$. The key factors in simulation performance using this approach are therefore simulation time, simulation bandwidth, and number of scatterers.

The memory requirements of the algorithm scale linearly with the number of signal samples. The size of the working set required by the simulator is constant and small—large data sets which do not fit in memory can be streamed from disk on demand with little performance loss.

On current PC hardware (Intel Core 2 Quad at 2.4 GHz), simulator execution requires about 1 s of run time per 5×10^6 samples, per target. Based on this performance, the simulation algorithm is practically applicable to most types of radar systems without requiring special purpose hardware. For example, simulation of a search radar with 50 targets, a bandwith of 25 MHz, a PRF of 400 Hz, and a pulsewidth of 10 μs can be performed approximately in real time on low-cost PC hardware.

In addition to good efficiency on general purpose computers, this algorithm is extremely easy to parallelise for operation on cluster supercomputers, specialised parallel computing hardware or commodity multi-core PC processors. Measurements on modern multi-core systems have revealed that performance scales approximately linearly with processor count as long as the number of processors is less than the number of required returns ($R \times T \times P$). The Karp-Flatt estimate of the serial portion for long pulse lengths approaches 11%.

The algorithm is also suitable for implementation on commodity graphics processors. Preliminary results suggest that parallel execution on a Nvidia 8800 GPU and the 2.2 GHz Athlon64 CPU can reduce simulation time by 60%.

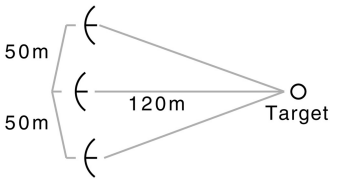

Fig. 4. Layout of netted radar system for verification experiments.

V. VERIFICATION OF SIMULATION ACCURACY

A. Implementation of Simulation Algorithm

The simulation approach described here has been implemented in a complete radar simulation system titled flexible extensible radar simulator (FERS). Implemented in portable C++, the simulator aims to be flexible through supporting runtime extensions written in the Python and C++ programming languages. The simulator has been released as open source software under the GNU General Public Licence [20]. Source code for this implementation can be freely obtained from http://www.sourceforge.net/projects/fers/.

B. Verification with Netted Radar

The first phase of verification of the accuracy of the simulation algorithm was performed using data from NetRad prototype netted radar system [7, 8], designed and operated by the Microwaves, Radar, and Optics group at University College London.

1) *Design of Radar Equipment and Experiments*: The prototype system used in the experiment consists of three nodes, which were arranged 50 m apart on an arc of radius 120 m, as illustrated in Fig. 4. The nodes are equipped with antennas with an azimuth beamwidth of approximately 30° and gain of 15 dBi. The antennas were aimed at the center of the arc of nodes.

In the experiment described here, 1.5 μs linear chirps with a bandwidth of 50 MHz were transmitted from each antenna in turn with nominal power of −23 dBm. All the nodes received and sampled the return pulse at 100 MHz.

Approximately 10 sets of data generated by this radar system have been compared with simulations performed using the FERS radar simulator. Two of these experiments are described in detail in this section, and the results are presented and discussed.

2) *Static Target Experiment*: In the first experiment, a static conductive cylindrical target with RCS of 0.6 m^2 was placed at the center of the arc.

Fig. 5 compares the simulated and actual system returns for a pulse transmitted from node 1 and

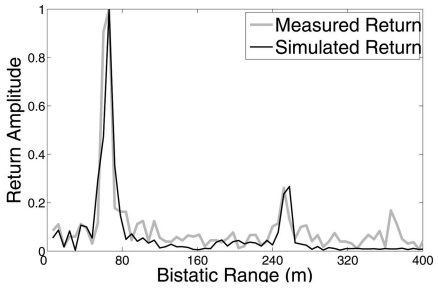

Fig. 5. Comparison of simulated bistatic radar response and return from prototype netted radar system.

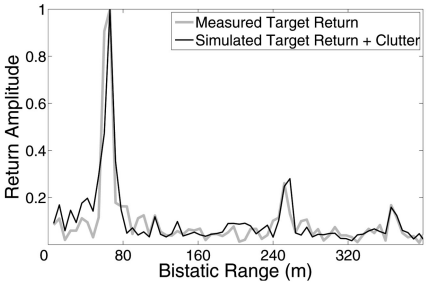

Fig. 6. Comparison of simulated bistatic radar response plus measured clutter and return from prototype netted radar system.

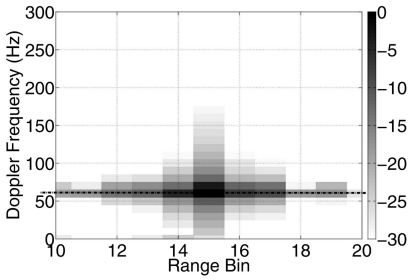

Fig. 7. Range/Doppler plot of results of moving target experiment measured with NetRad.

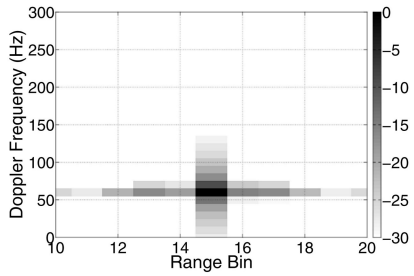

Fig. 8. Range/Doppler plot of results of simulation of moving target experiment.

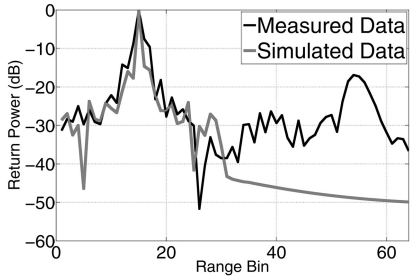

Fig. 9. Comparison of simulated and measured results in Doppler bin 7.

received at node 2. The data was pulse compressed for ease of comparison, and both simulated and actual returns were normalized to full scale. Two clear peaks are evident in both the measured and simulated return. The first of these, at approximately 50 m corresponds to the signal received at node 2 directly from node 1. The second peak, at approximately 250 m, corresponds to the return pulse from the cylindrical target.

Several peaks are visible in the measured return data which are absent in the simulated return data, especially above 320 m of range. These responses correspond to trees and other clutter present in the measurement range. Fig. 6 compares the measured system return (as in Fig. 5) with the sum of the simulated target return and measurements of the clutter present in the test range with no target in place.

These figures show a high degree of similarity between the measured and simulated results. The relative return powers from the target and direct signal between antennas was identical. The position of the target return and direct response peaks are similar between the measured and simulated targets with minor differences due to inaccuracies in the experimental setup.

3) *Moving Target Experiment*: In the second experiment, the static target was replaced with a truck driven at a nominal speed of 9 ms^{-1} obliquely across the range. The RCS of the target was approximately 10 m^2. In this experiment, transmissions were interleaved between the nodes for a total PRF of 20 kHz.

Figs. 7 and 8 present range/Doppler plots of the pulse compressed results of measurements and simulations, respectively. In both plots, clutter with zero Doppler has been suppressed to make the target more clearly visible. In the images, white corresponds to −30 dBm normalized return power and black to 0 dBm.

The overall structure of the results are very similar with the peak situated in the same range and Doppler bins, and a similar sidelobe structure along the range and frequency axes. The simulated results show stronger sidelobes in the frequency axis.

Fig. 9 illustrates the range versus return power in the Doppler bin 7. The line through which this slice is taken is marked with a dashed black line in Fig. 7. The overall structure of these results is extremely similar, showing the strong peak corresponding to the moving target. Clutter returns are present in the measured data beyond range bin 25, which are not evident in the simulated data.

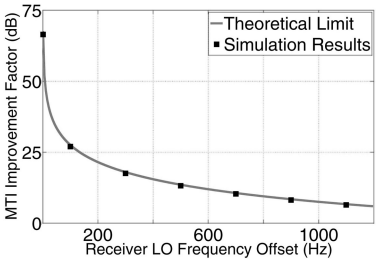

Fig. 10. MTI improvement factor (theoretical versus simulated) at range of 40 km.

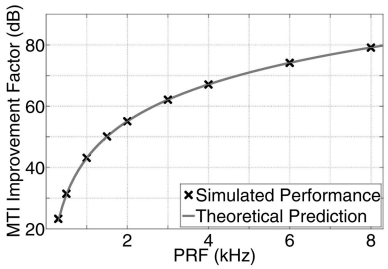

Fig. 11. MTI improvement factor (theoretical versus simulated) limit by scan modulation.

C. Comparison with Theoretical Performance of MTI Systems

A key step in the validation of the accuracy of a simulation system is the comparison of the simulation results with theoretical predictions. During the development and implementation of the model described in this paper, the results of processing simulation outputs were compared with theoretical predictions of the performance of radar systems.

Fig. 10 illustrates the results of one such experiment. The figure compares simulation results and theoretical predictions [21] for the MTI improvement factor of a single canceller MTI system in the presence of an offset in frequency between the transmitter and receiver local oscillators.

The results of an experiment comparing simulated versus theoretically predicted performance for an MTI system limited by antenna scan modulation is illustrated in Fig. 11. In this simulation, an antenna scan rate of 360°/s and an antenna with a Gaussian gain pattern and −3 dB beamwidth of 6° were chosen. Other system parameters were chosen to ensure that the improvement factor was limited by antenna scan modulation.

In each of these cases, it is clear that simulation results closely match theoretical predictions for simulations of the performance of MTI systems. Similar results for other types of radar processing have been achieved, including pulse-Doppler processing, SAR, and PCL-style [5] CW processing.

VI. CONCLUSIONS

A flexible model for signal-level simulation of diverse radar systems has been developed. This model and the related algorithms can be applied to simulate all key effects relevant to airborne and fixed radar systems, including designs such as netted and phased-array radars. The method described here is sufficiently efficient to run complex simulations on modern desktop computers in real time, and is suitable for implementation on dedicated DSP hardware for time critical applications.

Verification of the accuracy of simulation results is ongoing, but preliminary results, presented in this paper, suggest that this algorithm can simulate physical systems with excellent accuracy. Results of radar and sonar experiments demonstrate that the Doppler and phase shift simulation offered by the algorithm is accurate for sonar systems. We are confident that the ongoing verification with radar data will yield similarly encouraging results.

A. Future Work

The simulator currently supports only point scatterers with arbitrary multistatic RCS. While this is sufficient for many applications, simulation of complex target interactions would be useful in several radar fields, for example, micro-Doppler target identification, SAR, and ISAR systems. We are investigating the integration of existing finite element method (FEM) RF simulation codes for complete support of target modelling.

ACKNOWLEDGMENT

Thanks to Shaun Doughty and Professor Chris Baker at University College London for giving us access to results from the NetRad system.

REFERENCES

[1] Barton, D.
Modern Radar System Analysis.
Norwood, MA: Artech House, 1988.

[2] Franceschetti, G., Iodice, A., Perna, S., and Riccio, D.
Efficient simulation of airborne SAR raw data of extended scenes.
IEEE Transactions on Geoscience and Remote Sensing, **44**, 2 (2006), 2851–2860.

[3] Fabozzi, D., Franz, C., and Hancock, R.
High fidelity circular array simulation.
IEEE Aerospace and Electronic Systems Magazine, **22** (Dec. 2007), 11–17.

[4] Lengenfelder, R.
The design and implementation of a radar simulator.
M.S. thesis, University of Cape Town, Cape Town, South Africa, Sept. 1998.

[5] Griffiths, H. D. and Baker, C. J.
Passive coherent location radar systems: Part 1: Performance prediction.
IEE Proceedings—Radar, Sonar and Navigation, **152** (June 2005), 153–159.

[6] Baker, C. J., Griffiths, H. D., and Papoutsis, I.
Passive coherent location radar systems: Part 2: Waveform properties.
IEE Proceedings—Radar, Sonar and Navigation, **152** (June 2005), 160–168.

[7] Derham, T., Woodbridge, K., Griffiths, H., and Baker, C.
The design and development of an experimental netted radar system.
In *Proceedings of the International Radar Conference*, Sept. 2003, 293–298.

[8] Doughty, S. R.
Multistatic radar measurements and development.
M.S. thesis, University College London, London, UK, Dec. 2005.

[9] Dutre, P., Bala, K., and Bekaert, P.
Advanced Global Illumination.
Wellesely, MA: A K Peters, 2006.

[10] Shannon, C. E.
Communication in the presence of noise.
Proceedings of the Institute of Radio Engineers, **37** (Jan. 1949), 10–21.

[11] Smith, J. O. and Gossett, P.
A flexible sampling-rate conversion method.
In *Proceedings of the International Conference on Acoustics, Speech, and Signal Processing*, vol. 22, 20–23, 1974.

[12] Kaiser, J. F.
Using the I0 sinh window function.
IEEE Transactions on Circuits and Systems, **22** (1974), 20–23.

[13] Oppenheim, A. V., Schafer, R. W., and Buck, J. R.
Discrete-Time Signal Processing (2nd ed.).
Upper Saddle River, NJ: Prentice-Hall, 1999.

[14] Smith, J. O.
Digital Audio Resampling Home Page.
Available at http://wwwccrma.stanford.edu/~jos/resample/, Jan. 2002.

[15] Abramowitz, M. and Stegun, I. A.
The Handbook of Mathematical Functions.
Mineola, NY: Dover Publications, 1965.

[16] Widrow, B.
Statistical analysis of amplitude-quantized sampled data systems.
IEEE Transactions on Industry Applications, **81** (Jan. 1961), 555–568.

[17] Kester, W.
Analog-Digital Conversion.
Norwood, MA: Analog Devices, 2004.

[18] Brooker, M. and Inggs, M.
Efficient generation of f noise sequences for pulsed radar simulation.
IEEE Transactions on Aerospace and Electronic Systems, accepted for publication 2008.

[19] Hawksford, M. O. J.
Jitter simulation in high resolution digital audio.
Presented at the 121st Convention of the Audio Engineering Society, Oct. 2006.

[20] GNU
The GNU General Public License.
Available June 1991 at http://www.gnu.org/licenses/gpl.html.

[21] Kerr, R. R.
MTI Systems.
Norwood, MA: Artech House, 1993.

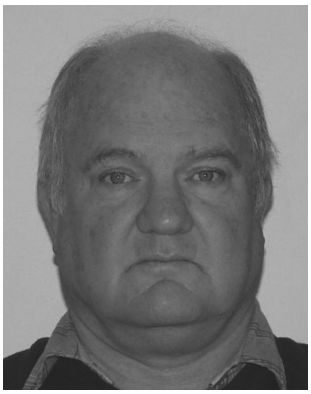

Michael Inggs (S'98) was born and educated in the Eastern Cape, South Africa (Uitenhage and Grahamstown). He has an Honours degree in physics and applied mathematics from Rhodes University (1973) and a Ph.D., D.I.C. from Imperial College, London (1979). He has worked in industry in the UK, USA, and South Africa, and joined the Department of Electrical Engineering, University of Cape Town in 1988, where he holds the rank of professor. He is a visiting professor at University College London and Liverpool Hope University. His research is in the area of radar, remote sensing, and high performance computing, and he is currently seconded part time to the South African Centre for High Performance Computing. He has more than 150 journal and conference publications, three patents, and has supervised more than 60 M.Sc. and 6 Ph.D. to completion.

Marc Brooker (M'02) received his B.Sc. (Eng.) in electrical and computer engineering from the University of Cape Town in 2005, and graduated with his Ph.D., also from UCT, in 2008. His Ph.D. research was into radar simulation, including the simulation of the effects of phase noise on the performance of multistatic radar systems.

Dr. Brooker is currently interested in parallel and highperformance computing, and works for Amazon.com.